Journal of Control, Automation and Electrical Systems (2020) 31:226–232
https://doi.org/10.1007/s40313-019-00536-0

Foundations on the Hamiltonian Energy Balance Method for Power System Transient Stability Analysis: Theory and Simulation

Emanuelle C. Machado[1,2] · **José E. O. Pessanha**[1]

Received: 30 April 2019 / Revised: 2 October 2019 / Accepted: 5 October 2019 / Published online: 21 October 2019

Abstract
Significant progress was made in the 1980s and 1990s in the development and application of direct methods in power system transient stability analysis. However, there is still certain mistrust because most of them have been built on heuristics, simplifications and simulations. To build confidence in direct energy methods, a first version of a Hamiltonian energy balance method based on perturbation theory and wave energy function was recently proposed. In this method, the kinetic and potential Hamiltonian energies of the dynamical system are computed in the prefault, fault-on and postfault periods, using the time-independent Schrodinger equation, canonical transformation and calculus of variations. One major disadvantage of the method is that it still does not compute the critical clearing angle (CCA) and the critical clearing time (CCT). In the present paper, earlier and current theoretical concepts built on a preliminary topological characterization of the stable equilibrium energy boundary (also referred to as energy barrier) are used to address this deficiency, resulting in a new version of the Hamiltonian energy balance method that is tested for computing CCA and CCT, providing more accurate results than other methods available in the literature.

Keywords Energy function · Hamiltonian formalism · Transient stability · Power systems

1 Introduction

Energy-based (Kakimoto et al. 1978; Pai 1982) direct methods can determine transient stability of power systems without the effort of indirect methods (time-domain simulations), providing a quantitative measure of the degree of system stability. This additional information makes direct methods very attractive when the relative stability of different network configuration plans must be compared or when operating limits constrained by transient stability must be calculated quickly. From an analytical viewpoint, these methods were originally developed for power systems with autonomous postfault systems. Essentially, there are several challenges and limitations involved in the practical applications of direct methods for power system transient stability analysis, some of which are inherent to these methods and some of which are related to their applicability to power system models (Chiang 2011; Pillco and Alberto 2015).

Regardless of the substantial progress over the last decades, direct methods are still considered not viable by many researches and engineers for power system applications. Recently, an energy balance method for direct analysis of transient stability, known as Hamiltonian energy balance function for power systems (HEBFPS) (Machado and Pessanha 2019), was proposed based on classical Hamiltonian formalism. The method has proven to be accurate and reliable based on preliminary results, mainly because it is free of heuristics, limitations and approximations, as normally seen in conventional methods (Chiang et al. 1987; Chiang 2011). Besides, a new concept of energy variables to the problem has been introduced, known as holonomic constraints (Meyer et al. 2009), which are the only variables that are actually used in the solution, reducing computational effort as fewer variables are required. It will be recalled that the transient stability problem had never been formulated through Hamil-

✉ José E. O. Pessanha
jeo.pessanha@ufma.br

Emanuelle C. Machado
elleuname321@gmail.com

[1] GASPSD - Group of Advanced Studies in Power Systems Dynamics, Federal University of Maranhao, São Luís, MA 65080-805, Brazil

[2] FAPEMA - State of Maranhão Research Foundation, São Luís, MA, Brazil

tonian formalism as shown in this paper, except in control (Liu et al. 2003, 2012; Sun et al. 2002).

The HEBFPS method (Machado and Pessanha 2019) computes stable, unstable and controlling unstable operating points. However, the only version available until now does not calculate the critical clearing angle (CCA) and the critical clearing time (CCT), two major concerns in transient stability problems. Based on that, the method had to be expanded to compute these quantities, as described in this paper. The proposal is tested and compared to other methods with two power systems. The results obtained with the proposed approach are promising and stimulating to implement new features and to conduct further investigations.

2 Computation of the Critical Clearing Time and Critical Clearing Angle

Earlier concepts of the HEBFPS method are very important to understand and to support the current work. Since important steps had to be summarized in (Machado and Pessanha 2019) for sake of space, some of them are expanded and clarified in the present paper. Let us first recall some aspects of the method that are useful to calculate the CCT and CCA, as seen next.

The final equilibrium (stable/unstable) of a power system has been determined based on a Hamiltonian energy balance approach (dimensionless) and on stability criteria, as given in (1) and (2), respectively. It will be recalled that stability criteria are built on exergy rate equations (Robinett and Wilson 2011), perturbation theory, wave energy function and dissipation-induced instabilities (Krechetnikov and Marsden 2007). The superscripts "0" and "PF" correspond to the prefault and postfault periods and "T" to the total energy balance.

$$\mathrm{d}H^T = \mathrm{d}H^0 + \mathrm{d}H^{\mathrm{PF}} \tag{1}$$

$$\begin{aligned} &\mathrm{d}H^T < 0, \text{ postfault stable} \\ &\mathrm{d}H^T > 0, \text{ postfault unstable} \\ &\mathrm{d}H^T = 0, \text{ at the boundary} \end{aligned} \tag{2}$$

To calculate CCT and CCA, the fault-on Hamiltonian energies $\left(\mathrm{d}H^F\right)$ must be determined at each time interval $(t_0 < t < t_{\mathrm{cl}})$. First, it is necessary to calculate the fault-on holonomic constraints $\left(\delta^F, \omega^F\right)$ of the generator (classical model), which amount will depend on the number of integration intervals ($i = 1, 2, \ldots, n$), as shown in Fig. 1. The fault-on holonomic constraints are used for the computation of the fault-on Hamiltonian energies, which in turn are used to calculate the CCA and the CCT.

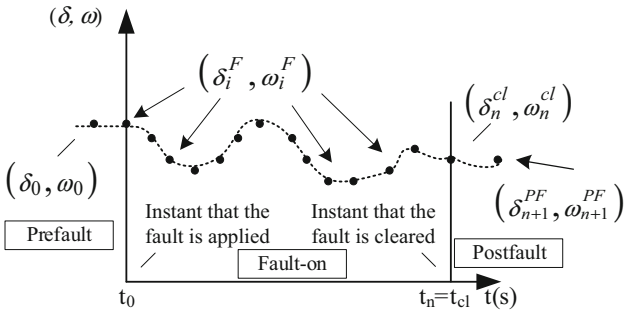

Fig. 1 Holonomic constraints' dynamics

There is a major difference between the first version of the method and the current one. Originally, the fault-on Hamiltonians have been intended only to the computation of the postfault Hamiltonian, as shown in (1). Since we want to calculate the CCT and the CCA, we just need to know the fault-on Hamiltonians, from the moment that the fault is applied (t_0) to the moment that is cleared (t_{cl}). This change may be easily understood based on the explanation given below.

If a fault is applied at t_0, and as long as it lasts, the Hamiltonian energy of the generator will change because of the variations of the holonomic constraints and of its output electric power. The equilibrium now is computed as shown in (3), i.e., the energy balance uses the Hamiltonian energy calculated at the instant that the fault is cleared.

$$dH^T(t) = dH^0(t_0) + dH^F(t_{cl}) \tag{3}$$

It is easily noticed that both CCT and CCA must be computed when (3) equals zero, the third stability criterion of (2). Such a situation occurs when $\mathrm{d}H^F = \mathrm{d}H^0$ with opposite signs ($\pm$), recalling that stable energy regions are always characterized by $(\mathrm{d}H(t_i) < 0)$, while unstable regions by $(\mathrm{d}H(t_i) > 0)$. Based on that, there are two ways to compute CCA and CCT: (i) monitoring the fault-on Hamiltonians until it equals prefault or (ii) monitoring the fault-on Hamiltonian energy balance (computed at each time interval) until it equals zero. The first results in less computational cost, and it is therefore considered here. Besides, it should be avoided that the total Hamiltonian energy balance (3) becomes positive, which would be probably too late to prevent the generator from operating unstable, and consequently, the computation of CCT and CCA under this condition is not justified.

Algorithm Computation of the critical clearing angle and critical clearing time via HEBFPS method.

First step: Compute P_m^0 and P_e^0 through power flow analysis. The holonomic constraints δ^0 and ω^0 are computed

in the same way as in time-domain analysis for the initial conditions.

Second step: Construct the prefault Hamiltonian energy function (4) using the values computed in step 1.

$$H^0\left(\delta^0,\omega^0\right)=\underbrace{\left(p_0^2/2\mu\right)}_{H^0_{\mathrm{KE}}(\omega_0)}+\underbrace{\left[P_m^0-P_e^0\left(\delta^0\right)\right]}_{H^0_{\mathrm{PE}}(\delta_0)} \tag{4}$$

The prefault conjugate momentum (p_0) of the generator is given in (5), and therefore, the kinetic energy is expressed by (6).

$$p_0=\partial H/\partial\dot{\delta}=\mu\dot{\delta};\quad \dot{\delta}=p_0/\mu \tag{5}$$

$$H^0_{\mathrm{KE}}=p_0^2/2\mu \tag{6}$$

Third step: Compute the prefault Hamiltonian energy (7)–(9) using function (4).

$$\mathrm{d}H^0=\left(-\partial H_0/\partial\delta_0\right)\mathrm{d}\delta_0+\left(\partial H_0/\partial p_0\right)\mathrm{d}p_0 \tag{7}$$

$$-\partial H_0/\partial\delta_0=-\partial/\partial\delta_0\left[p_0^2/2\mu+\left[P_m^0-P_e^0\right]\right]=-\partial P_e^0/\partial\delta_0 \tag{8}$$

$$\partial H_0/\partial p_0=\partial/\partial p_0\left[p_0^2/2\mu+\left[P_m^0-P_e^0\right]\right]=p_0/\mu \tag{9}$$

Fourth step: Construct the fault-on Hamiltonian energy function (10). It will be recalled that i is the number of fault-on integration intervals ($i=1,2,\ldots,n$).

$$H^F\left(\delta_i^F,\omega_i^F\right)=\underbrace{\left(p_i^2/2\mu\right)}_{H^F_{\mathrm{KE}}(\omega_i^F)}+\underbrace{\left[P_m-P_{e_i}^F\left(\delta_i^F\right)\right]}_{H^F_{\mathrm{PE}}(\delta_i^F)} \tag{10}$$

Fifth step: Simultaneous computation of the fault-on holonomic constraints of the generator and its output electric power $\left(\delta_i^F,\omega_i^F,P_{e_i}^F\right)$ in the time domain and of the fault-on "F" Hamiltonians for each interval t_i according to (11)–(13), using function (10).

$$\mathrm{d}H_i^F=\int_{t_0}^{t_{\mathrm{cl}}}\left(\partial H_i^F/\partial t\right)\mathrm{d}t \tag{11}$$

$$\partial H_i^F/\partial p=\partial/\partial p\left[p_i^2/2\mu+\left[P_m-P_{e_i}^F\left(\delta_i^F\right)\right]\right]=p_i^F/\mu \tag{12}$$

$$-\partial H_i^F/\partial\delta=-\left(\partial/\partial\delta\right)\left[p_i^2/2\mu+\left[P_m-P_{e_i}^F\left(\delta_i^F\right)\right]\right]=-\partial P_{e_i}^F/\partial\delta \tag{13}$$

Sixth step: Compute the total "T" Hamiltonian energy balance at the instant that the fault is cleared $-t_n=t_{\mathrm{cl}}$ (14).

$$\mathrm{d}H^T=\mathrm{d}H^0+\mathrm{d}H_n^{\mathrm{cl}} \tag{14}$$

Seventh step: Determine the postfault equilibrium state of the power system according to the criteria described in (2).

Eighth step: Compute CCT and CCA with (15)–(18).

$$t_{\mathrm{cr}}=\int_{t_0}^{t_i}\int_{t_i}^{t_{\mathrm{cl}}}\underbrace{\left(\partial\dot{H}_i^F/\partial t\right)}_{\mathrm{d}\dot{H}_i^F}\underbrace{\left(\frac{\partial H_i}{\partial t_i}-\mathrm{d}H_i\right)}_{\Delta\dot{H}_i^F}\mathrm{d}\delta$$

$$=\int_{t_0}^{t_{\mathrm{cl}}}\left[\left(\mathrm{d}\dot{H}_i^F\right)\Delta\dot{H}_i^F\right]\mathrm{d}(\Delta\delta) \tag{15}$$

$$\delta_{\mathrm{cr}}=\int_{\delta_0}^{\delta_i}\int_{\delta_i}^{\delta_{\mathrm{cl}}}\underbrace{\left(\partial\dot{H}_i^F/\partial t\right)}_{\mathrm{d}\dot{H}_i^F}\underbrace{\left(\frac{\partial H_i}{\partial t_i}-\mathrm{d}H_i\right)}_{\Delta\dot{H}_i^F}\mathrm{d}\delta$$

$$=\int_{\delta_0}^{\delta_{\mathrm{cl}}}\left[\left(\mathrm{d}\dot{H}_i^F\right)\Delta\dot{H}_i^F\right]\mathrm{d}(\Delta\delta) \tag{16}$$

$$\frac{\partial\left(\Delta\dot{H}_i^F\right)}{\partial\delta}=\frac{\partial}{\partial\delta}\left[\frac{\mathrm{d}}{\mathrm{d}t}\left(\Delta H_i^F\right)\right]=\left(\mu\ddot{\delta}_i^F\right)-\frac{\partial P_{e_i}^F\left(\Delta\delta_i^F\right)}{\partial\delta} \tag{17}$$

$$\ddot{\delta}_i^F\approx\lim_{\omega_0\to\Delta\omega_i}\left(\Delta\dot{\omega}_i^F\right)\approx\lim_{\omega_0\to\Delta\omega_i}\left(\frac{\omega_i-\omega_0}{\Delta t}\right) \tag{18}$$

Some steps must be taken to improve accuracy and reliability of the proposed method, as shown in (15) and (16), in which the dynamic trajectory of the fault-on Hamiltonian energy from prefault (t_0), up to the instant that the fault is cleared (t_{cl}), is approximated by very small pieces, using the partition path integral over a chosen interval $[\Delta\delta,\Delta t]$ technique (Gonzalez 2000). It must be recalled that the fault-on Hamiltonian is monitored until $\mathrm{d}\dot{H}_i^F=\mathrm{d}H^0$, exactly when the balance is zero $\left(\mathrm{d}H(t_i)=\mathrm{d}H^0+\mathrm{d}H_i^F=0\right)$. Theoretically, both CCA and CCT are computed under such conditions. Computationally, we might have to assume the closest values because of the approximate integration technique

The previous algorithm has been described for the classical generator model only, but it can be easily extended for any machine model just adding new holonomic constraints to the energy functions. Besides, if only the total energy balance is of interest, step 8 is skipped.

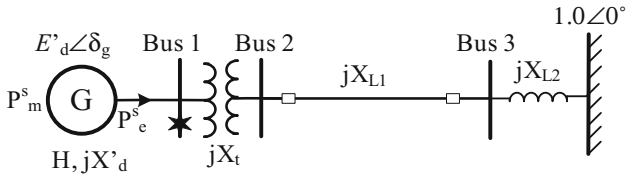

Fig. 2 Single-machine infinite bus

3 Application of the Method

Let us illustrate the application of the method considering the single-machine infinite-bus test system (SMIB) shown in Fig. 2. A three-phase short circuit is applied at the generator's terminals (Bus 1). The system's data have been taken from Padiyar (2008): $jX'_d = 0.3$ pu, $jX_t = 0.1$ pu, $jX_{L1} = 0.4$ pu, $jX_{L2} = 0.1$ pu, $P_e^0 = 1.0$ pu, $H = 4$ and $f = 50$ Hz. It will be recalled that the method normally does not use the moment of inertia (M) of the generator, but its inertia tensor (μ) instead. Here, since the system comprises just one generator, it is correct to assume $\mu \cong H = 4$. A fault-on period of 0.1105 s has been chosen to compute CCT and CCA. Some steps of the algorithm were put together in the analysis as follows:

(a) Initial conditions (step 1).

$$P_m = 1.0 \text{ pu } P_e^0 = 1.0 \text{ pu } \delta^0 = 51.17^\circ \ \omega^0 = 314.16 \text{ rd/s}$$

(b) Computation of the prefault Hamiltonian energy (steps 2 and 3).

$$\mathrm{d}H^0 = \left(-\partial H_0/\partial \delta_0\right)\mathrm{d}\delta_0 + \left(\partial H_0/\partial p_0\right)\mathrm{d}p_0 = -2.083$$

(c) Computation of the fault-on Hamiltonian energy (steps 4 and 5). The time interval must be chosen in such a way that $\mathrm{d}H_i^F \cong \mathrm{d}H^0$ can be computed.

$$\mathrm{d}H_i^F = \int_0^{0.1103} \left(\partial H_i^F/\partial t\right)\mathrm{d}t = +2.397$$

(d) Computation of the energy balance at the instant that the fault is cleared ($t_{\mathrm{cl}} = 0.1103$ s) (step 6).

$$\mathrm{d}H^T = -2.083 + 2.507 = +0.424$$

(e) Since $\mathrm{d}H^T = +0.424 > 0$, the system is unstable according to the criteria presented in (2) (step 7). The analysis would end here if no further computations had been required.

(f) Due to the fact that the total balance is positive, it means that the clearing time 0.1103 s is above critical time. The angle at this instant has been computed as 64.63° (1.1280 rds). It is clear that both CCT and CCA are less than these computed values.

Table 1 Fault-on Hamiltonians and corresponding time interval

$\mathrm{d}H_i^F$	Time interval [0, 0.1105]	Angle interval [0.8931, 1.1280]
+ 1.094	0.1096	1.1259
+ 1.391	0.1097	1.1266
+ 1.558	0.1098	1.1270
+ 1.736	0.1099	1.1275
+ 2.083	0.1100	1.1277
+ 2.149	0.1101	1.1279
+ 2.205	0.1102	1.1280
+ 2.397	0.1103	1.1259

(g) Integrals (15) and (16) are solved using the partition path integral technique over the intervals [0, 0.1103] and [0.8931, 1.1280], respectively (step 8).

$$t_{\mathrm{cr}} = \int_0^{0.1103} \left[\left(\mathrm{d}\dot{H}_i^F\right)\Delta\dot{H}_F\right]\mathrm{d}t$$

$$\delta_{\mathrm{cr}} = \int_{0.8931}^{1.1280} \left[\left(\mathrm{d}\dot{H}_i^F\right)\Delta\dot{H}_i^F\right]\mathrm{d}(\Delta\delta)$$

It is exactly at $\mathrm{d}\dot{H}_i^F \cong \mathrm{d}H^0$ that the critical clearing time and the critical clearing angle must be taken. The results are given in Table 1 using four-digit decimal arithmetic, where the critical clearing time and critical clearing angle are 0.1100 s and 1.1277 rds, respectively. The results are in good agreement with those obtained by (Padiyar 2008).

Figure 3 shows the 3D Hamiltonian energy balance storage surfaces of the previous example. In the prefault period, the Hamiltonian balance is inside a basin of attraction, as shown in Fig. 3a, and therefore, the system is stable. In the fault-on period and until the fault is cleared, the energy of the system is deformed because of the degenerative nature of the fault energy. When the fault is cleared at the critical time, the Hamiltonian is still inside the basin of attraction, as shown in Fig. 3b, and the system remains stable. For a clearing time greater than the critical time, the Hamiltonian leaves the basin of attraction and lies in an unstable region, as shown in Fig. 3c. The previous computation of the critical clearing time and critical clearing angle has been corroborated through the 3D Hamiltonian energy balance storage surfaces.

The above examples have just illustrated the proposed approach step by step. In real simulations, as seen next, the method computes the final energy balance, the critical clearing time and the critical clearing angle without forced interruptions.

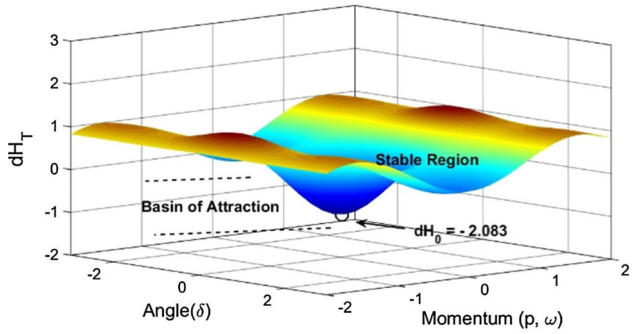

(a) Prefault – power system is stable

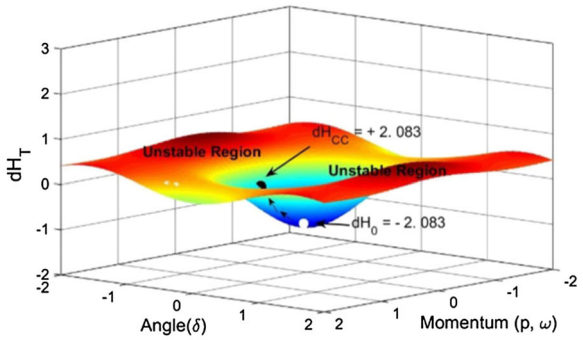

(b) Critical clearing time - power system remains stable

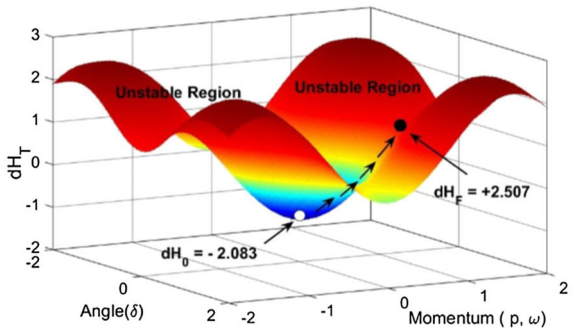

(c) Over critical clearing time - power system is unstable

Fig. 3 3D energy storage surface of the generator

4 Computer Simulations

The proposal is now evaluated with two power systems and compared to other methods available in the literature. The code has been designed in MATLAB—version 2016a, and runs on a Desktop PC—Intel Core™ i7, 4790 3.60 GHz CPU 16.0 GB RAM, 64 bits. The simulations data can be found in the respective references.

(a) Test System I—WSCC 9-bus 3-machine
The method is first tested with the WSCC 3G 9-bus power system, taken from (Chiang 2011), where the author applies the network-reduction BCU method. On the other hand, there are no reductions nor simplifications of any kind in the proposed method, without compromising computational efficiency (low CPU time) and accuracy of results. The classical model with a uniform damping factor represents all generators, and the loads are of constant impedance type. The results presented in Table 2 are in good agreement with BCU method, which version is the one used in (Chiang 2011).

(b) Test 50G—145-bus power system model
The critical clearing time is now computed for the 50G—145-bus power system (Vittal 1992; Chiang 2011). The main objective is to verify the accuracy of the method through comparative analysis. Table 3 provides the computed CCTs in ms by five different methods and for different faults (Chiang 2011). As can be seen, the results are very accurate, being the closest ones to time domain in six simulations out of eight (except for a fault at buses 91 and 33).

The Hamiltonian energy balances have been computed for the first fault (bus#7), as given in Table 4. For sake of space, only the energy balances of the most critical generators to the fault, G20 and G26, are presented. The system is prefault stable, as well as postfault when the fault is cleared at $t_{\mathrm{cl}} = 0.1080s$, because $\mathrm{d}H_0$ and $\mathrm{d}H_T$ are negative. In this case, G20 and G26 present the lowest negative energy balances (close to zero and to the energy boundary). On the other hand, the system is postfault unstable when the fault is cleared at $t_{\mathrm{cl}} = 0.1085s$, because all $\mathrm{d}H_T$ are positive. In this case, G20 and G26 present the highest positive energy balances. (The energy boundary has already been crossed.) The results in terms of equilibrium are in good agreement with those presented in (Vittal 1992).

5 General Remarks

Current energy-based methods normally provide information on transient stability problems via specific energy indexes, where the most common are: stable equilibrium points (SEPs), closest unstable equilibrium points (UEPs) and controlling unstable equilibrium points (CUEPs), besides the critical fault clearing time and the critical generator's angle (Owusu-Mireku and Chiang 2018; Tang et al. 2018). It was not found it necessary to perform in the present paper the computations of SEPs, UEPs and CUEPs, since they can be found in Machado and Pessanha (2019). Here, most of the results obtained with the proposed method for calculating CCT and CCA (Sect. 4) were closer to those obtained in the time domain.

The current approach is still built on the original Hamiltonian energy balance method, in a manner not seen so far.

Table 2 Critical clearing time and critical clearing angle—WSCC *power system*

(contingency #) Fault at bus#/ opened line		CCT (s)			CCA (in radians) $\delta_1/\delta_2/\delta_3$	
		HEBFPS	BCU	Time domain	HEBFPS	BCU
(1) 4	4–6	0.32	0.31	0.32	−0.0317 0.0951 0.0501	−0.0319 0.0949 0.0492
(2) 5	5–7	0.33	0.33	0.33	−0.1202 0.3390 0.2236	−0.1204 0.3394 0.2239
(3) 6	6–9	0.33	0.34	0.34	−0.0966 0.2180 0.2957	−0.0967 0.2180 0.2958
(4) 7	7–8	0.36	0.35	0.36	−0.0655 0.2429 −0.0023	−0.0655 0.2430 −0.0024
(5) 8	8–9	0.27	0.26	0.27	−0.0461 0.0725 0.2080	−0.0462 0.0728 0.2082

Table 3 CCTs (ms) computed with different methods

Fault at bus#/ opened line		Method				
		HEBFPS	Time domain	BCU	MOD	Exit point
7	7–6	107.5	108.2	102.0	112.5	112.5
73	73–84	211.1	215.5	194.2	**	**
91	91–75	187.7	188.0	187.7	187.5	187.5
66	66–67	170.6	171.0	163.5	**	**
33	33–39	384.7	386.0	385.0	**	347.5
69	69–32	203.4	205.3	186.2	**	**
59	59–103	220.2	222.6	220.0	**	242.5
105	105–73	212.8	213.5	206.5	**	**

**Unsolved

Table 4 Hamiltonian energy balances

Gen	dH^0	$t_{cl} = 0.1080s$ stable		$t_{cl} = 0.1085s$ unstable	
		dH^F	dH^T	dH^F	dH^T
G20	− 3.094	+ 2.739	− 0.355	+ 10.518	+ 7.424
G26	− 3.094	+ 1.183	− 1.911	+ 6.240	+ 3.146

It will be recalled that the Hamiltonian energy functions are formulated based on the holonomic constraints (δ, ω) of the generator (classical model). It means that information on the angle of the generator, one of the main concerns of the problem, can be obtained from the related formulations, as shown in Sects. 2 and 3.

6 Conclusions

A reformulated version of the Hamiltonian energy balance method including the computation of the critical clearing time and the critical clearing angle, quantities that were not computed in the original version, is presented and described in this paper. Due to the fact that the main foundations of the method have been kept, the new version is also free of the limitations, heuristics and challengers normally found in conventional energy-based methods. Besides, for achieving high accuracy, the partition path integral technique has been applied for solving the critical clearing time and critical clearing angle integrals. The proposal has been validated and compared to other methods available in the literature. Preliminary tests indicate that the proposal gives the most accurate results in the estimated CCTs and CCAs. The approach is very sensitive to any change in the energy of the system, capturing information on the degeneration of the prefault energy caused by the destructive nature of the fault energy. It is very likely that the method will be appropriate for online transient stability assessment, after further investigations, improvements and tests.

Funding This work was supported in part by the State of Maranhão Research Foundation (FAPEMA) under Grant BD-01478/19.

References

Chiang, H. D. (2011). *Direct methods for stability analysis of electric power systems: Theoretical foundation, BCU methodologies, and applications* (1st ed.). Hoboken: Wiley.

Chiang, H. D., Wu, F., & Varaiya, P. (1987). Foundations of direct methods for power system transient stability analysis. *IEEE Transactions on Circuits and Systems, 34*(2), 160–173.

Gonzalez, O. (2000). Time integration and discrete Hamiltonian systems. In *Journal of nonlinear science mechanics: From theory to computation* (pp. 257–275). New York: Springer.

Kakimoto, N., Ohsawa, Y., & Hayashi, M. (1978). Transient stability analysis of electric power system via lure-type Lyapunov function—part I new critical value for transient stability. *IEE J, 98,* 63–71.

Krechetnikov, R., & Marsden, J. E. (2007). Dissipation-induced instabilities in finite dimensions. *APS Reviews of Modern Physics, 79*(2), 519–553.

Liu, H., Hu, Z., & Song, Y. (2012). Lyapunov-based decentralized excitation control for global asymptotic stability and voltage regulation of multi-machine power systems. *IEEE Transactions on Power Systems, 27*(4), 2262–2270.

Liu, Q. J., Sun, Y. Z., Shen, T. L., & Song, Y. H. (2003). Adaptive nonlinear co-ordinated excitation and STATCOM controller based on Hamiltonian structure for multimachine-power-system stability enhancement. In *IEE proceedings—control theory and applications* (vol. 150, no. 3, pp. 285–294).

Machado, E., & Pessanha, J. E. O. (2019). Hamiltonian energy-balance method for direct analysis of power systems transient stability. *IET Generation, Transmission and Distribution, 13*(10), 1895–1905.

Meyer, K., Hall, G., & Offin, D. (2009). *Introduction to Hamiltonian dynamical systems and the N-body problem* (1st ed.). New York: Springer.

Owusu-Mireku, R., & Chiang, H.-D. (2018). A direct method for the transient stability analysis of transmission switching events. In *Proceedings IEEE PESGM, Portland*, pp. 1–5.

Padiyar, K. R. (2008). *Power system dynamics stability and control* (2nd ed.). Hyderabad: BS Publications.

Pai, M. A. (1982). *Energy function analysis for power system stability*. Boston: Kluwer Academic Publishers.

Pillco, E. C., & Alberto, L. F. C. (2015). Direct methods for stability assessment of two-time-scale electrical power system models. In *2015 IEEE Eindhoven PowerTech, Eindhoven*, pp. 1–6.

Robinett, R. D., III, & Wilson, D. G. (2011). *Nonlinear power flow control design: Utilizing exergy, entropy, static and dynamic stability, and Lyapunov analyses* (1st ed.). Berlin: Springer.

Sun, Y. Z., Liu, Q. J., Song, Y. H., & Shen, T. L. (2002). Hamiltonian modelling and nonlinear disturbance attenuation control of TCSC for improving power system stability. *IEE Proceedings—Control Theory and Applications, 149*(4), 278–284.

Tang, Y., Li, F., Wang, Q., & Xu, Y. (2018). Hybrid method for power system transient stability prediction based on two-stage computing resources. *IET GTD, 12*(8), 1697–1703.

Vittal, V. (1992). Transient stability test systems for direct stability methods. *IEEE Transactions on Power Systems, 7*(1), 37–43.